

Mapping and Characterization of Iron-Containing Particles in Brain Tissue

A. Mikhailova,¹ M. Davidson,² Y. Guyodo,³ H. Tostmann,⁴
J. Culp,⁴ J. Dobson,⁵ R. Duran,⁴ J. Channell,³ C. Batich¹

¹ Biomedical Engineering Department, University of Florida, Gainesville, FL, U.S.A.

² Microfabritech, University of Florida, Gainesville, FL, U.S.A.

³ Geology Department, University of Florida, Gainesville, FL, U.S.A.

⁴ Chemistry Department, University of Florida, Gainesville, FL, U.S.A.

⁵ Dept. of Biomedical Engineering and Medical Physics, Keele University, Stoke-on-Trent, United Kingdom

Introduction

We are presently developing a method for high-resolution structural iron mapping in brain tissue. Analysis of iron in tissue is normally investigated by histochemical or microscopy methods. In recent studies, Mössbauer spectroscopy and micro particle-induced x-ray emission (micro-PIXE) were used for multi-elemental analysis of plaques in brain tissue.¹ Collective data from those studies determines the cellular distribution of iron deposits and its elemental content. Here we describe the use of x-ray fluorescence (XRF) and EXAFS for high-resolution, chemical-state-specific iron assay in brain tissue using an avian brain tissue model. The high sensitivity of XRF allows rapid location of very small particles of iron oxide crystallites using a large analysis

Materials and Methods

X-ray absorption spectra were recorded in fluorescent and transmission modes at Sector 10 (MRCAT) available to the University of Florida at the Advance Photon Source (APS) at Argonne National Laboratory. The beam size was $\approx 150\text{-}200\ \mu\text{m}$ vertically and horizontally, which corresponds to $150\ \mu\text{m}$ resolution. A schematic representation of the station is given in Fig. 1. Figure 2 is a picture of the experimental setup.

Pigeon brains were used as an animal model by choice as it has been shown in other studies that this bird possesses super-

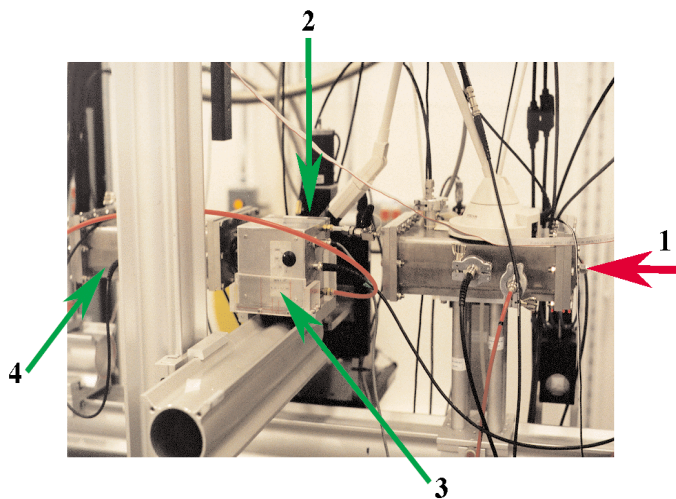


FIG. 1. Picture of experimental setup.

area, followed by further refinement of the location by successively smaller analysis areas. This technique is used to produce maps of iron anomalies in the tissue based on iron oxidation state which is characterized by Fe-K-edge XANES spectra. This approach presents a challenge, as XANES/XAFS spectra measured by x-ray fluorescence strongly depends on the concentration of the element, thickness of the sample, and detection geometry resulting from the self-absorption effect. These experiments were designed to detect iron-containing anomalies by observation of the Fe absorption edge at a well-defined energy and to determine the structure by comparison of the positions of the absorption edge and the shapes of pre-edge and edge regions of detected anomaly with known standard samples. In addition, detailed analysis of the EXAFS data obtained from the iron anomalies found in the tissues is providing clues to the structure and source of the iron crystallites.

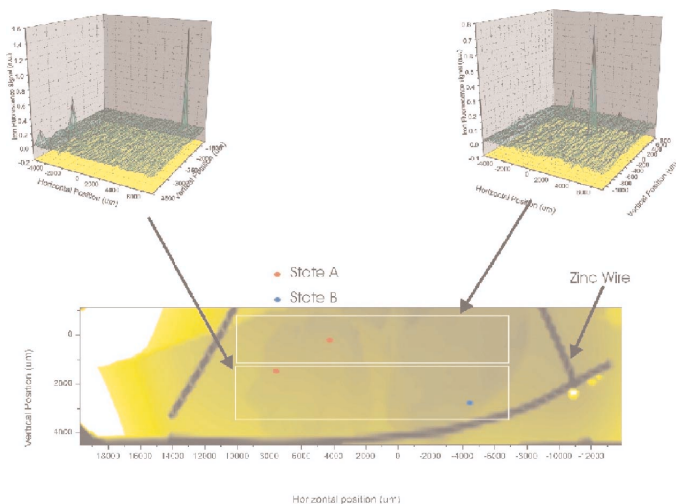


FIG. 2. Area scans of overall tissue showing transmission image and two iron fluorescence maps.

paramagnetic biogenic magnetite particles in the head as a part of a magnetoreceptor system. Tissue samples were fixed by immersion in 2% buffered glutaraldehyde, cut into sections $45\text{-}50\ \mu\text{m}$ thick, postfixing in osmium tetroxide, gradually dehydrated, and flat embedded in TAAB epoxy resin (Malovax Inc.) between two Kapton (Dupont) sheets. For biological standards, we used a bacterial culture of *Magnetospirillum magnetotacticum* (ATCC), horse spleen ferritin, pigeon hemoglobin, and the heme-part of cytochrome purchased from Sigma-Aldrich.

Each specimen was initially screened by line scans for iron using a $500\ \mu\text{m}$ pixel size. The region of the tissue samples with detected iron was then raster scanned at $200\ \mu\text{m}$ pixel resolution. More detailed mapping was done to determine the exact location of iron anomalies. X-ray absorption spectra were collected at each of the anomalies and XANES/XAFS data were used to determine the iron species.

XAFS analysis was accomplished using WinXAS software for plotting and data reduction,² FEFF7, and FEFFIT for fitting to crystallographic information to XAFS data.³

Results and Discussion

A typical area scan of a pigeon brain section is shown in Fig. 2. The lower image is a transmission map of the fixed and mounted pigeon brain section. The two hemispheres of the brain section can be clearly seen, as well as the outline of a 10 mil zinc wire embedded in the epoxy with the tissue. The zinc wire serves as a spatial reference, allowing precise location of the particles found using the XRF mapping in later, more conventional microscopic analysis. The two maps shown above the transmission image are iron XRF maps with the Z-axis representing the magnitude of the fluorescence signal change from below the iron absorption edge to above the absorption edge energy. There are three clearly identifiable iron particles in this particular sample. Note that conventional elemental mapping techniques cannot be used for finding these particles due to the extremely low number density of particles within the brain combined with the small particle size (typically <1 μm).

A typical EXAFS spectrum obtained from one of these particles is shown in Fig. 3. The spectrum is shown overlaid with a spectrum of magnetite obtained from the magnetotactic bacteria. The spectra are quite similar. The inset shows the overlaid spectrum of ferritin, a common iron storage protein. The ferritin spectrum is similar in major features to the magnetite; however, the smaller features appear to be different. The ferritin molecule typically has a core crystallite consisting of hydrated iron oxide with a structure typical of ferrihydrite.⁴ The ferrihydrite structure contains both octahedrally and tetrahedrally coordinated iron atoms. XAFS simulations have been completed on magnetite and the two iron sites in ferrihydrite. One of the ferrihydrite iron sites yields an XAFS spectrum very similar to the magnetite. The second iron site is quite different. Further refinements of the models and fitting to the reduced $\text{Chi}(k)$ XAFS data is in progress.

Acknowledgments

Use of the Advanced Photon Source was supported by the U.S. Department of Energy, Office of Science, Office of Basic

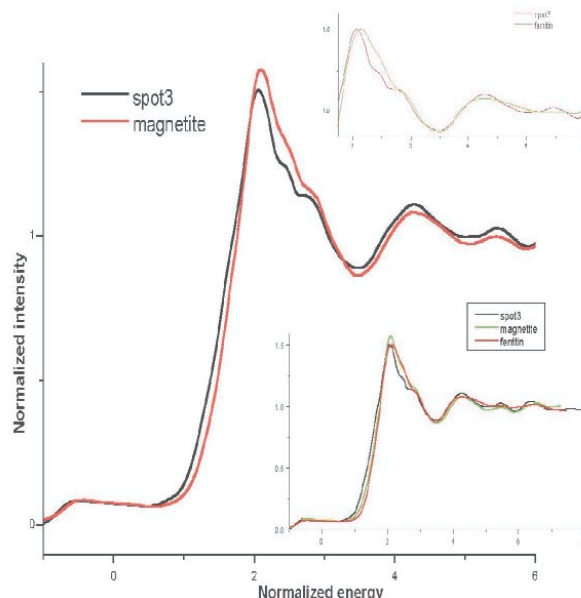


FIG. 3. Typical XAFS spectrum of iron oxide particle tentatively identified as magnetite.

Energy Sciences, under Contract No. W-31-109-ENG-38 and the Materials Research Collaborative Access Team. This research program is supported by the University of Florida, Office of Research, Technology, and General Education.

References

- ¹ J. Makjanic; F. Watt, Nuclear Instruments & Methods in Physics Research, Section B: Beam Interactions with Materials and Atoms **150**, 167-172, (1999).
- ² T. Ressler, J. Physique IV, **7**, C2-269 (1997).
- ³ S.I. Abinsky, J.J. Rehr, A. Ankudinov, R.C. Albers, M.J. Eller, Phys. Rev. B, **52**, 2995 (1995).
- ⁴ J.M. Crowley, D.E. Janney, R.C. Gerkin, and P.R. Buseck, *Journal of Structural Biology* **131**, 210-216 (2000).